Brief communication

n/p-Type changeable semiconductor TiO$_2$ prepared from NTA

Qiuye Li, Xiaodong Wang, Zhensheng Jin*, Dagang Yang, Shunli Zhang, Xinyong Guo, Jianjun Yang and Zhijun Zhang
*Key Laboratory of Special Functional Materials, Henan University, Kaifeng, 475001, China; *Author for correspondence (Tel.: +86-378-2852533; Fax: +86-378-2852533; E-mail: zhenshengjin@henu.edu.cn)*

Abstract

A novel kind of nano-sized TiO$_2$ (anatase) was obtained by high-temperature (400–700°C) dehydration of nanotube titanic acid (H$_2$Ti$_2$O$_4$(OH)$_2$, NTA). The high-temperature (400–700°C) dehydrated nanotube titanic acids (HD-NTAs) with a unique defect structure exhibited a p-type semiconductor behavior under visible-light irradiation ($\lambda \geq 420$ nm, $E_{photon} = 2.95$ eV), whereas exhibited an n-type semiconductor behavior irradiated with UV light ($\lambda = 365$ nm, $E_{photon} = 3.40$ eV).

In 1998, Kasuga et al. reported a nanotube material obtained by treating anatase TiO$_2$ powder with a 5–10 M NaOH aqueous solution at 110°C (Kasuga et al., 1998, 1999; Zhang et al., 2000). This material was found to be nanotube sodium titanate (Na$_2$Ti$_2$O$_4$(OH)$_2$), which can be converted to NTA in a pH 1 HCl solution, and its crystalline form belongs to an orthorhombic system (Yang et al., 2003). Recently, above titanate nanotubes began to attract wide attention because of their potential applications in many areas such as photocatalysts (Hodos et al., 2004; Xu et al., 2005), ion exchangers (Sun & Li, 2003; Ma et al., 2005), a new generation of electrodes for lithium batteries (Kavan et al., 2004; Li et al., 2005a, b), adsorbents, and drug delivery materials.

It is well known that the surface/bulk structure and physico-chemical properties of TiO$_2$ can be greatly influenced by preparing methods. It is surprising, when NTA was annealed at high temperature, a novel kind of TiO$_2$ with special semiconducting property was obtained. Although this novel kind of TiO$_2$ has identical anatase crystal form to that of the raw material, it possesses a unique defect structure.

The preparation of NTA has reported elsewhere (Yang et al., 2003). The transmission electron microscopic (TEM) image of NTA is shown in Figure 1a. Its differential scanning calorimetric (DSC) spectrum (Figure 1b) can be divided into two temperature regimes partitioned by ca. 300°C:

i. at $T < 300$°C, only endothermic dehydration process took place;
ii. at $T > 300$°C, compared with X-ray diffraction (XRD) patterns (Figure 1c), it can be seen that the transformation of crystal form from orthorhombic NTA to anatase TiO$_2$ happened, that was an exothermic process peaked at 384°C (Figure 1b). In Figure 1c, when the dehydration temperature (T) moved from 400 to 700°C, the crystallinity of TiO$_2$(anatase) was enhanced, while the morphological changes simultaneously occurred, i.e. nanotubes were broken and gradually agglomerated into ellipsoidal nanoparticles (Figure 1d).
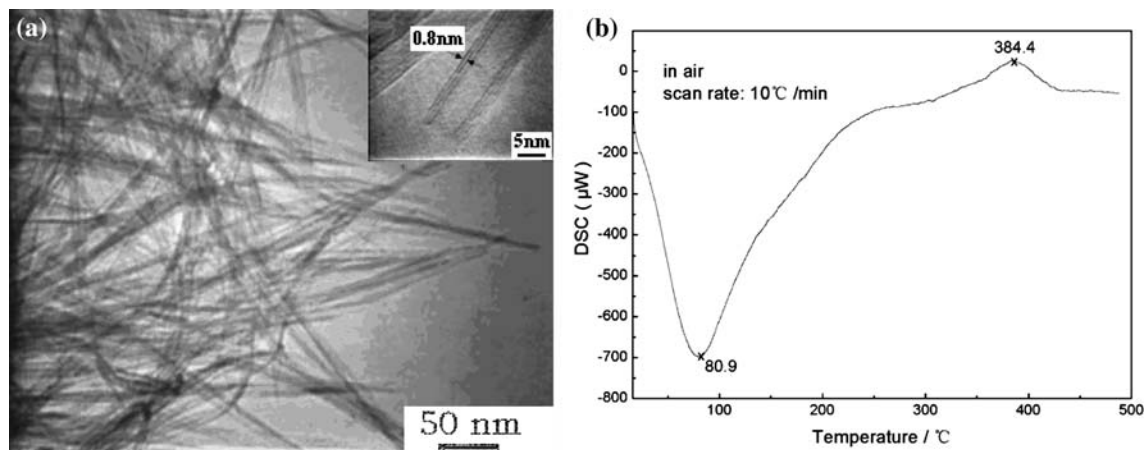
Figure 1. Preparation conditions of NTA and HD-NTAs: as prepared nanotube $Na_2Ti_2O_4(OH)_2$ were washed with deionized water to neutral pH, and then immersed in a 0.1 M HCl solution for 5 h, washed again with deionized water to remove Cl^-, and dried under vacuum (−0.1 MPa) at room temperature (20°C). HD-NTAs were obtained by annealing NTA in tubular oven at 400–700°C for 2 h, respectively. (a) TEM picture of NTA. Insert shows a four-layered nanotube with inner and outer diameters of 6.4 and 9.3 nm, respectively, the distance between two adjacent layers is ca. 0.8 nm. (b) DSC spectrum of NTA. (c) XRD patterns of NTA and HD-NTAs. (d) TEM images of HD-NTAs dehydrated at different annealing temperatures. From 400 to 700°C, the nanotubes were broken and gradually agglomerated into ellipsoidal nanoparticles (e) HRTEM picture for 600°C-dehydrated NTA. Rows point out the positions of defects. The d-spacing of 0.35 nm corresponds to the (110) plane of anatase.

HRTEM picture for 600°C-dehydrated sample shows a lot of defects to exist in the crystal lattice of anatase phase (Figure 1e).

The photoelectrochemical behaviors of high-temperature (400–700°C) dehydrated nanotube titanic acids (HD-NTAs) were studied. Using Degussa p-25 TiO_2 (n-type semiconductor) as reference, we found that under visible-light irradiation ($\lambda \geq 420$ nm, $E_{photon} = 2.95$ eV), HD-NTAs exhibited p-type semiconductor behavior, their open-circuit-photovoltage values are positive. In Figure 2a, $I_{photo}-V_{bias}$ curves indicate that the flat-band potential for the p-type HD-NTAs situates at +0.1 V, where at $V_{bias} < 0.1$ V, $I_{photo} < 0$; at $V_{bias} \geq 0.1$ V, $I_{photo} \approx 0$. On the contrary, when HD-NTAs were irradiated with UV light ($\lambda = 365$ nm, $E_{photon} = 3.40$ eV), they exhibited an n-type semiconductor behavior, their open-circuit-photovoltage values are negative. In Figure 2b, $I_{photo}-V_{bias}$ curves indicate that the flat-band potential for the n-type HD-NTAs situates at −0.7 V, where within $V_{bias} = -0.7$ to −0.4 V, I_{photo} increases with V_{bias}; at $V_{bias} > -0.4$ V, I_{photo} approaches to a steady value. Above results suggest that, when +0.1 V > V_{bias} > −0.7 V, the

semiconducting type of HD-NTA can be controlled by light, i.e. p-type by visible-light, n-type by UV light. A typical result for the n/p type-changeable semiconductor HD-NTA is shown in Figure 2c. After the dark current (I_{dark}) was stabilized (−0.7 ± 0.1 eV), the 1st-run and 2nd-run results were determined, where I = current determined, photo current (I_{photo}) = $I - I_{dark}$. It is evident that such an n/p type-changeable HD-NTA can be possibly used as a photo-switched material.

Electron spin resonance spectra (ESR) results proved that a large amounts of single electron-trapped oxygen vacancy (SETOV) formed in HD-NTA (Serwicka et al., 1981; Serwicka, 1985; Linsebigler et al., 1996). Each SETOV has one effective positive charge (denoted as V_o°). In Figure 3a–d, the unsymmetrical ESR signal ($g_\perp = 2.005$, $g_{//} = 1.985$) is resulted from the strong interaction between V_o°s (Su, 1987; Zhang et al., 2004a), the signal height is proportional to the concentration of SETOV (denoted as h_{SETOV}) (Su, 1987). The h_{SETOV} changes with T (Figure 3e).

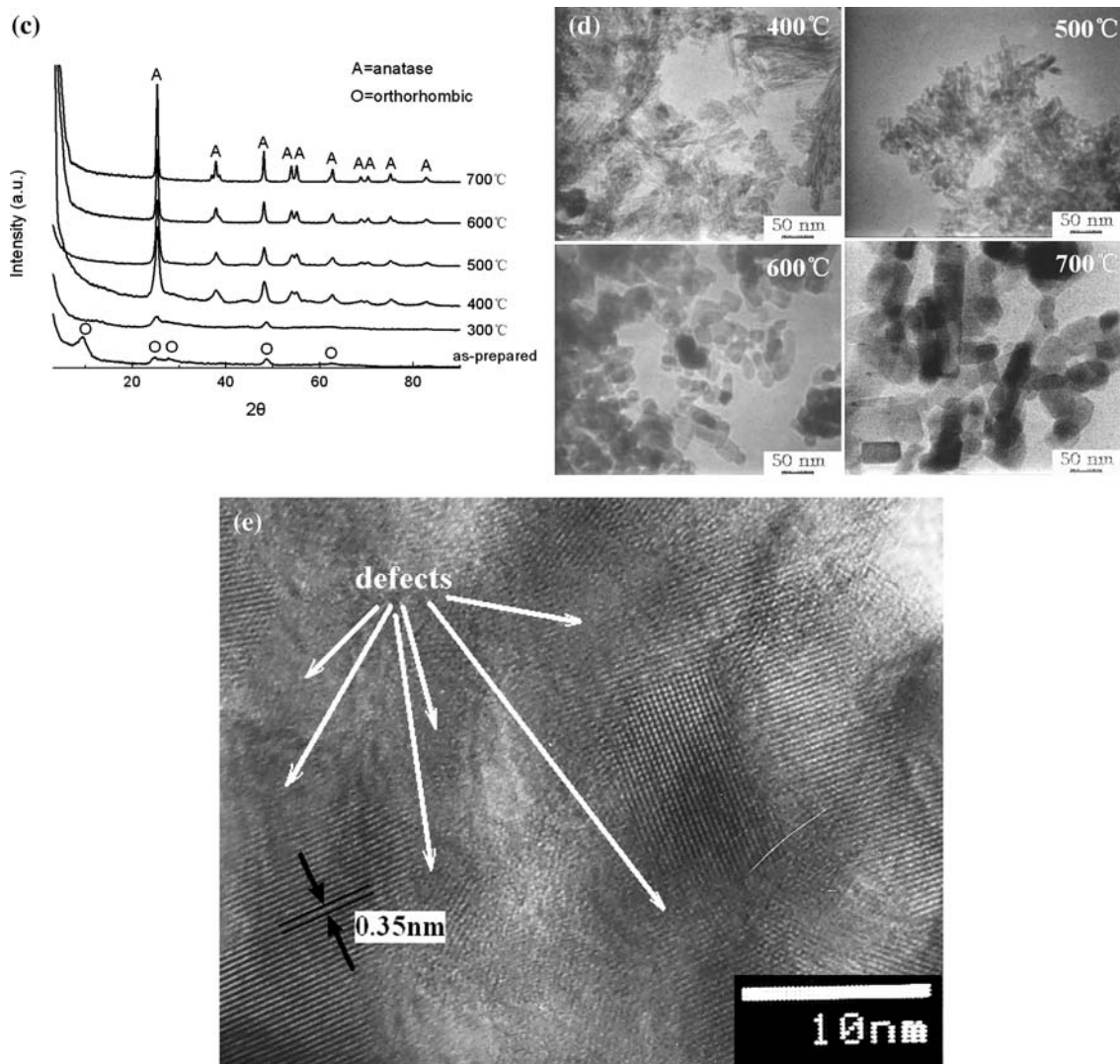Diffusion reflectance spectra (DRS) of as-prepared NTA and HD-NTAs are shown in

Figure 1. Continued.

Figure 4a. In DRS spectra, a strong absorption at $\lambda \leq 393$ nm indicates that the band gaps (E_g) of these samples are identical ($E_g = 3.15$ eV). However, in the DRS spectra of HD-NTAs the absorption at $\lambda > 400$ nm appears. According to KM theory, the absorption is proportional to $F(R'_\infty) = (1 - R'_\infty)^2 / 2R'_\infty$ (R'_∞ = reflectance) (Wendlandt & Hecht, 1966; Anderson & Pratt, 1985; Zhang et al., 2004b). Plot $F(R'_\infty)$ with T, the curve shown in Figure 4a inset is similar to both h_{SETOV}–T curve (Figure 3e) and inversed I_{photo}–T curve (Figure 2a inset), they all have a maximum at $T = 600°C$. Based on above results, we can

conclude that the p-type behavior of HD-NTAs must correlated to the sub-band structure induced by V_o°s within E_g (Qian et al., 2005). So the visible-light photon can be absorbed by V_o° to lift the trapped electron to conduction band and by valence band electron to transfer to oxygen vacancy. The former transition is a necessary prerequisite for the latter transition. It is well known that a depletion layer is necessary for the creation of an electric field, which separates electron-hole pairs (Gerischer, 1983). Under visible light illumination ($E_{photon} < E_g$) and at $V_{bias} < +0.1$ V, V_o°s will play the role of positive
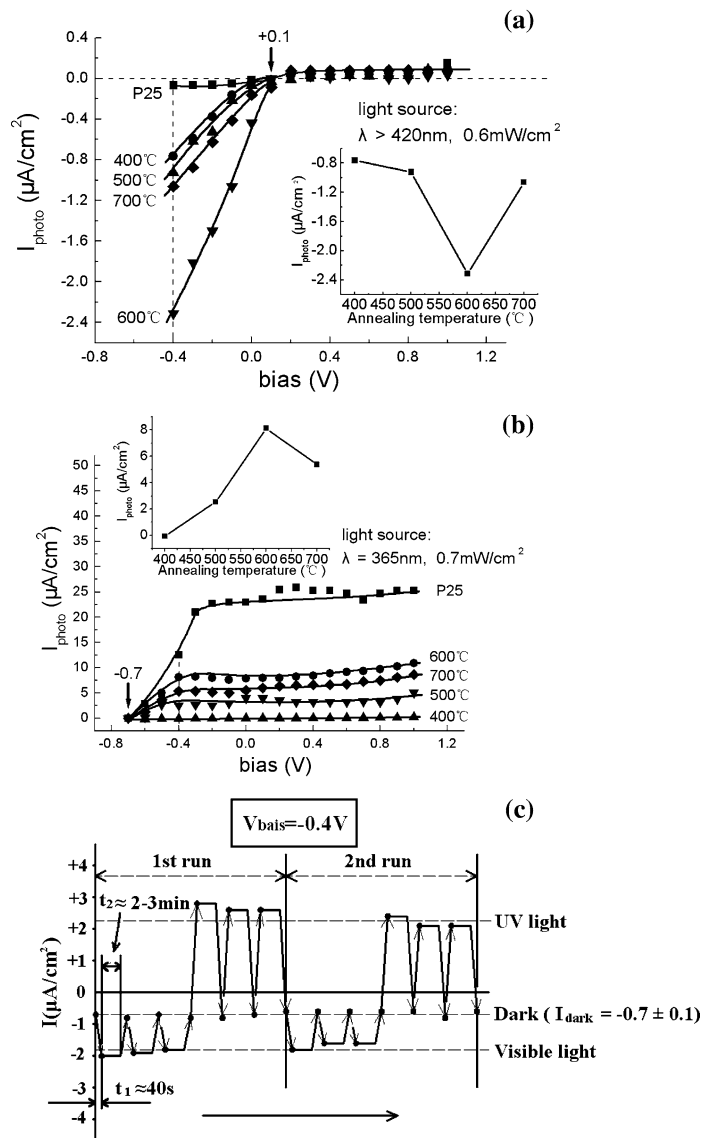
Figure 2. Photoelectrochemical behaviors of HD-NTAs. Photoelectrochemical measurements were conducted in a quartz cell consisted of a three-electrode system, where a standard calomel electrode (SCE) was used as the reference electrode and a 0.1 mol/l Na_2SO_4 solution as the supporting electrolyte. The working electrodes were prepared as follows: 1.0×1.0 cm ITO glasses ($R_\square = 80$ Ω/sq) were washed ultrasonically by ethanol, acetone and three-time distilled water in sequence, then baked in a muffle furnace at 450°C for 1 h. Aliquots of the dilute suspensions (2 g/l) of HD-NTAs were dropped on to ITO glasses, then dried under an IR lamp. This process was duplicated by five times. The counter electrode was Pt. (a) under visible-light irradiation. (b) Under UV irradiation. Insets of (a) and (b) show the $I_{photo}-T$ curves, respectively. (c) A typical result for the n/p type-changeable semiconductor HD-NTA. t_1 denotes the time from light-on to a steady current value. t_2 denotes the duration of the constant current, then light off.

majority carriers like h^+ to provide HD-NTA with a p-type semiconductor behavior (see Figure 4b model).

As pointed above, the visible-light photons can be successively absorbed by V_o° and by the valence-band electron. On 532 nm-laser illumination, the
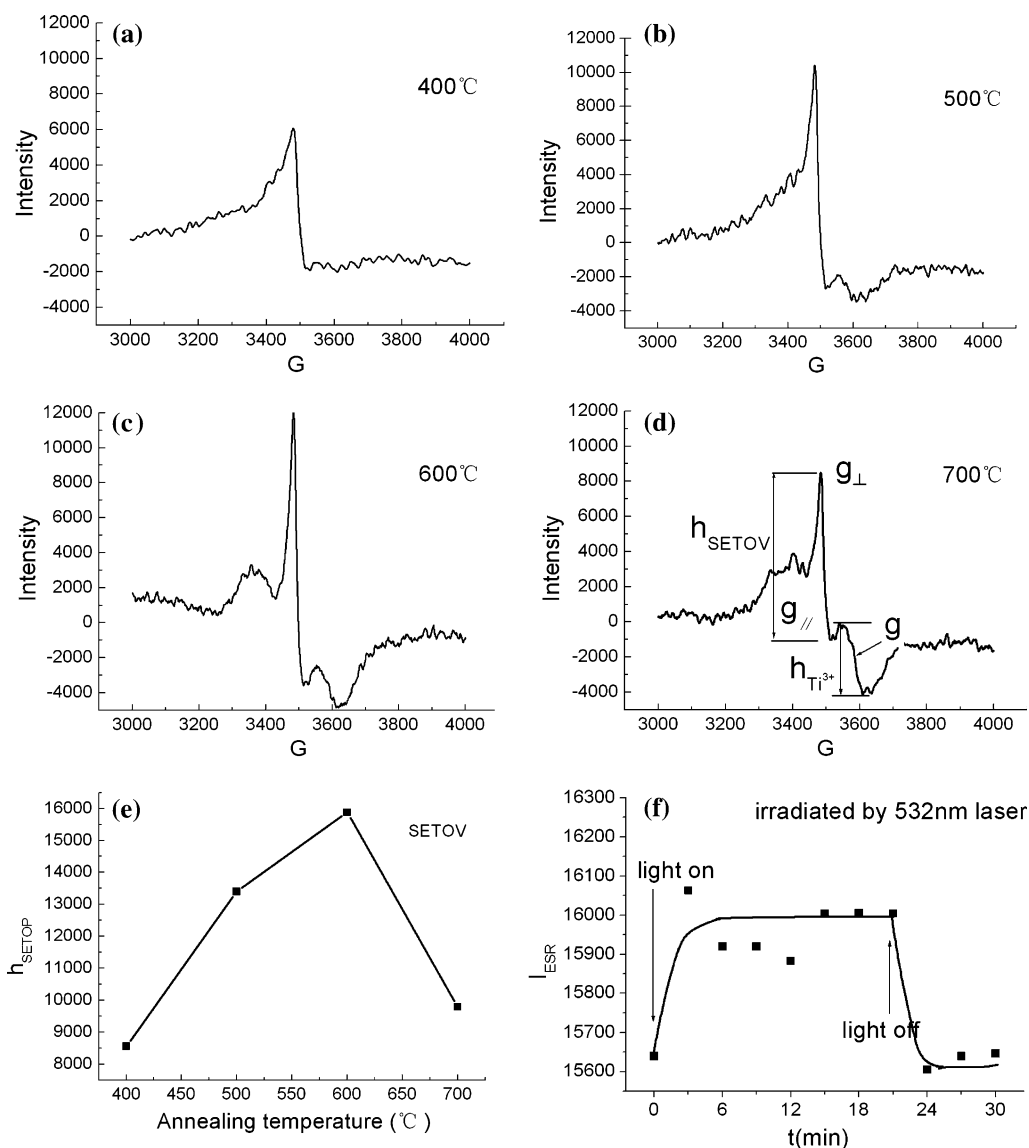
Figure 3. ESR results of HD-NTAs. ESR were obtained on a Brüker ESP 300E spectrometer which was operated in the X band (ca. 9.80 kHz) with 100 kHz field modulation, 0.2 mT amplitude modulation and 10 mW microwave power. *G* values were measured by taking diphenyl picryl hydrazyl ($g = 2.0036$) as a reference at room temperature (20°C). (a–d) ESR spectra of HD-NTAs. (e) Changes of concentration of SETOV (h_{SETOV}) with annealing temperature of HD-NTAs. (f) Changes of h_{SETOV} under 532 nm-laser illumination and in the dark.

concentration of SETOV should keep unchanged. However, Figure 3f shows that h_{SETOV} increases to a steady value, while in the dark it comes back to the initial level. This phenomenon hints that there are doubly ionized oxygen vacancies ($V_o^{\circ\circ}$) existed in HD-NTA. Each $V_o^{\circ\circ}$ can accept one electron from valence band to form one V_o°, thus, the

increasing of h_{SETOV} happened. Since it is reversible, h_{SETOV} came back to the initial level as the laser light turned off. In ESR spectra (Figure 3b–d), we also find Ti^{3+} signal ($g = 1.972$) (Che & Bond, 1985; Serwicka, 1985; Hirakawa et al., 2001). The appearance of Ti^{3+} and $V_o^{\circ\circ}$ in HD-NTAs evidences that the following reactions took
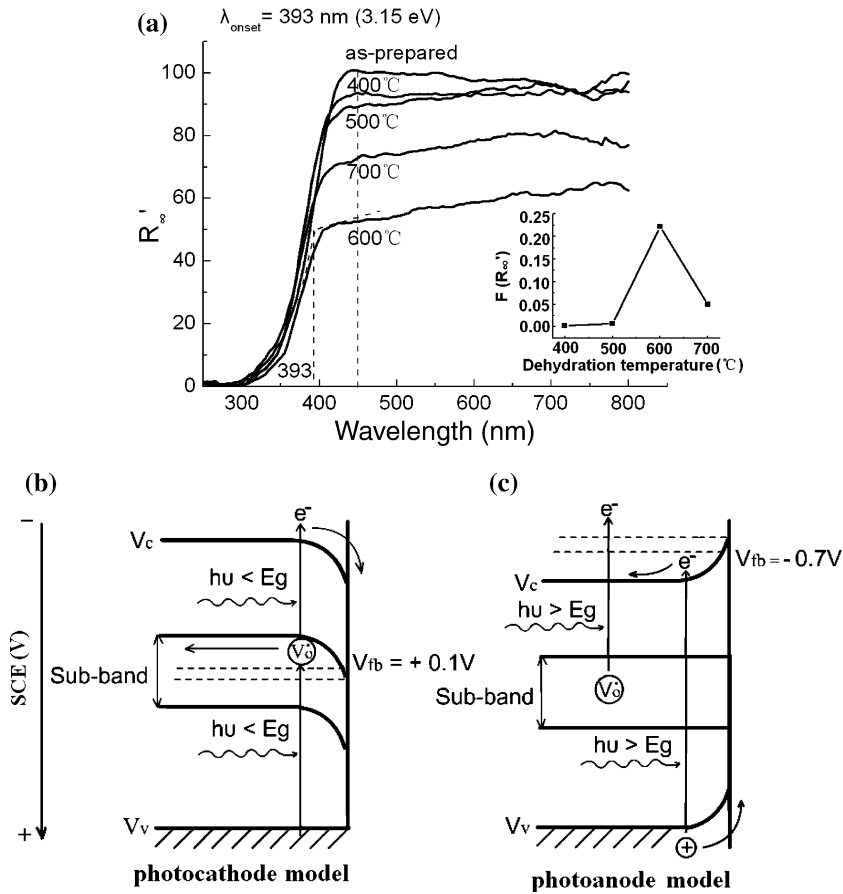
Figure 4. (a) Diffusion reflectance spectra (DRS) of as-prepared NTA and HD-NTAs. Inset shows the curve of $F(R'_\infty)$ with T. $F(R'_\infty) = (1-R'_\infty)^2/2R'_\infty (R'_\infty =$ reflectance). (b) Photocathode model of HD-NTA. Under visible light illumination, HD-NTA exhibits a p-type semiconductor behavior. (c) Photoanode model of HD-NTA. On UV light illumination, HD-NTA shows an n-type semiconductor behavior.

place during high-temperature annealing of NTA:

$$H_2Ti_2O_4(OH)_2 \rightarrow 2TiO_2 + 2H_2O + mV_O^\circ \quad (1)$$

$$V_O^\circ + Ti^{4+} \rightarrow V_O^{\circ\circ} + Ti^{3+} \quad (2)$$
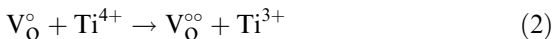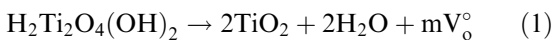
At $T \geq 600°C$ the V_O° formation ended (reaction 1), while reaction (2) still proceeded. It explains why h_{SETOV} has a maximum at $T = 600°C$ (Figure 3e), and h_{Ti}^{3+} increases with T (see Figure 3a–d).

On UV light illumination ($E_{photon} > E_g$) and at $V_{bias} > -0.7 V$, the valence-band electrons of HD-NTA can be directly excited to conduction band to show an n-type behavior(see Figure 4c model). Due to the trapped electron in oxygen vacancy can also be excited to conduction band

to increase the concentration of negative majority carriers e^-, i.e. to raise I_{photo}. So, the $I_{photo}-T$ curve shown in Figure 2b inset also has a maximum at $T = 600°C$.

In summary, we have obtained a novel kind of nano-sized TiO_2 (anatase) with a unique defect structure, which can be possibly used as a photo-switched material.

Acknowledgments

References

Anderson J.R. & K.C. Pratt, 1985. Introduction to Characterization and Testing of Catalysts. Australia: Academic Press.

Che, M. & G.C. Bond, (eds.), 1985. Adsorption and Catalysis on Oxide Surfaces. Amsterdam – Printed in The Netherlands: Elsevier Science Publishers B.V.

Gerischer H., 1983. Chemistry for the Futrue. Pergamon Press, Oxford, pp. 11–21.

Hirakawa T., H. Kominami, B. Ohtani & Y. Nosaka, 2001. J. Phys. Chem. B 105, 6993–6999.

Hodos M., E. Horváth, H. Haspel, Á. Kukovecz, Z. Kónya & I. Kiricsi, 2004. Chem. Phys. Lett. 399, 512–515.

Kasuga T., M. Hiramatsu, A. Hoson, T. Sekino & K. Niihara, 1998. Langmuir 14, 3160–3163.

Kasuga T., M. Hiramatsu, A. Hoson, T. Sekino & K. Niihara, 1999. Adv. Mater. 11, 1307–1311.

Kavan L., M. Kalbac, M. Zukalova, I. Exnar, V. Lorenzen, R. Nesper & M. Graetzel, 2004. Chem. Mater. 16, 477–485.

Li J., Z. Tang & Z. Zhang, 2005a. Electrochem. Commun. 7, 62–67.

Li J., Z. Tang & Z. Zhang, 2005b. Electrochem. Commun. 7, 894–899.

Linsebigler A., G. Lu Jr. & J.T. Yates, 1996. J. Phys. Chem. 100, 6631–6636.

Ma R., T. Sasaki & Y. Bando, 2005. Chem. Commun. 948–950.

Qian L., Z.S. Jin, J.W. Zhang, Y.B. Huang, Z.J. Zhang & Z.L. Du, 2005. Appl. Phys. A 80, 1801–1805.

Serwicka E., 1985. Colloids Surf. 13, 287–293.

Serwicka E., M.W. Schlierkamp & R.N. Schindler, 1981. Z. Naturforch. 36a, 226–232.

Su M., 1987. Solid State Chemistry, an Introduction. Beijing: Peking University Press (in Chinese).

Sun X. & Y. Li, 2003. Chem. Eur. J. 9, 2229–2238.

Wendlandt W.W. & H.G. Hecht, 1966. Reflectance Spectroscopy. New York: Wiley Interscience.

Xu J.C., M. Lu, X.Y. Guo & H.L. Li, 2005. J. Mol. Catal. A 226, 123–127.

Yang J., Z. Jin, X. Wang, W. Li, J. Zhang, S. Zhang, X. Guo & Z. Zhang, 2003. Dalton Trans. 3898–3901.

Zhang S., J. Zhou, Z. Zhang, A.V. Vorontsov & Z. Jin, 2000. Chin. Sci. Bull. 45(16), 1533–1536.

Zhang M., Z. Jin, J. Zhang, X. Guo, J. Yang, W. Li, X. Wang & Z. Zhang, 2004a. J. Mol. Catal. 217, 203–210.

Zhang S., W. Li, Z. Jin, J. Yang, J. Zhang, Z. Du & Z. Zhang, 2004b. J. Solid State Chem. 177, 1365–1371.